Electronic Supplementary Material (ESI) for Physical Chemistry Chemical Physics.

In situ electrochemical Raman investigation of charge storage in rGO and N-doped rGO

Rohit Yadav*, Prerna Joshi, Masanori Hara, and Masamichi Yoshimura

Graduate School of Engineering, Toyota Technological Institute, Nagoya, 468-8511, Japan.

E-mail: sd19503@toyota-ti.ac.jp

List Figures: **Page No.**

Tables: **Page No.**

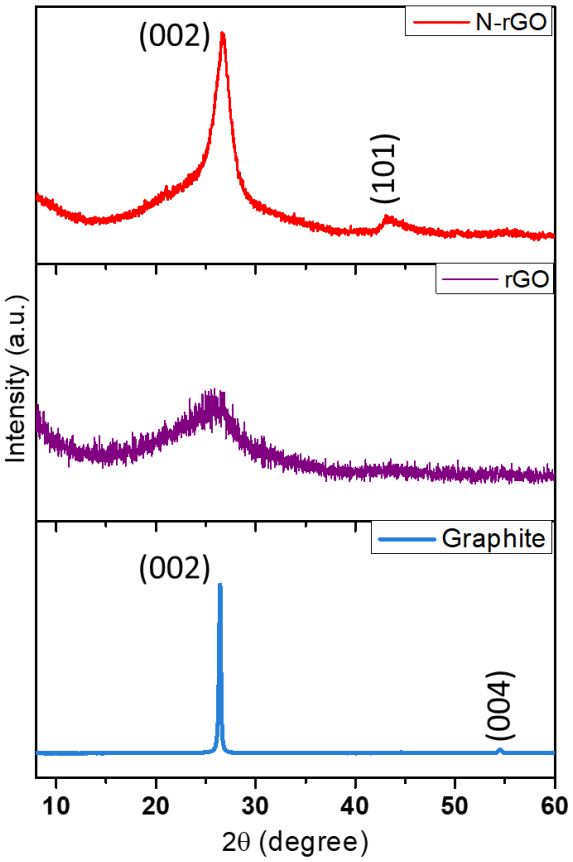

Fig. S1 XRD patterns of synthetic graphite, rGO, and N-rGO

Fig. S1 shows the characteristic peak corresponding to 002 plane in the XRD spectra at 2θ= 26.4, 25.8, and 27 degrees for synthetic graphite, rGO, and N-rGO, respectively. The 002 plane signifies the ordered stacking of graphene sheets. The sharp peak in graphite corresponded to its crystalline nature and ordered stacking of graphene sheets, whereas in rGO and N-rGO, broad 002 peak with a low intensity related to their exfoliated and smaller crystallite sizes due to structural defects from pyrolysis. Diffraction plane 101 and 004 represented different structural phases of graphene with corresponding interplanar distances, however, the intensity of the planes was very low for interpretation.

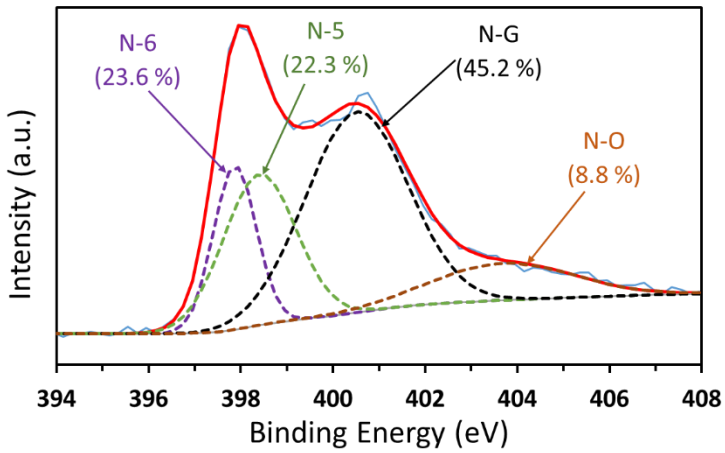

Fig. S2 XPS N 1s spectrum of N-rGO (solid line) and deconvolutes peaks (dashed lines) of four type of functionalities, pyridinic N (N-6), pyrolic N (N-5), graphitic N (N-G), and N oxide (N-O)

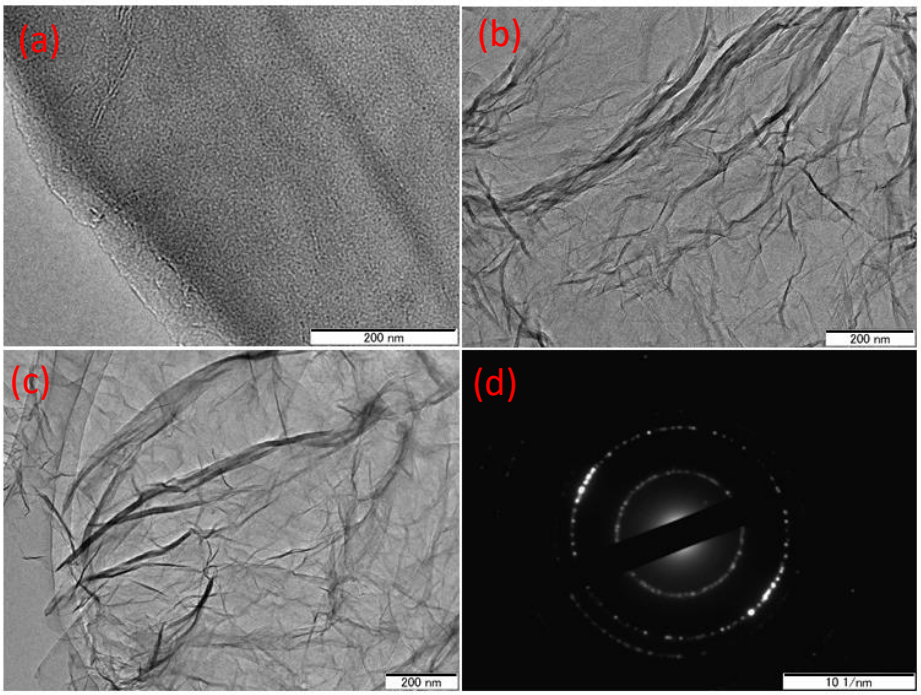

Fig. S3 TEM micrographs of (a) synthetic graphite, (b) rGO, (c) N-rGO, and (d) Selected area electron diffraction (SAED) of synthetic graphite,

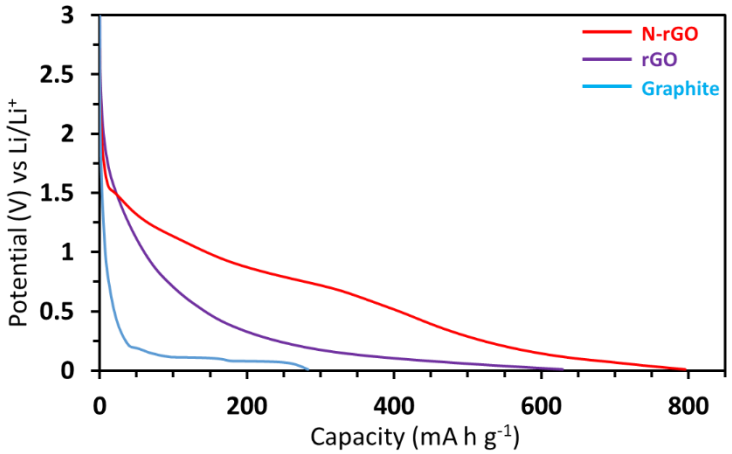

Fig. S4 First charge profile of synthetic graphite, rGO, and N-rGO electrode at C/15 rate

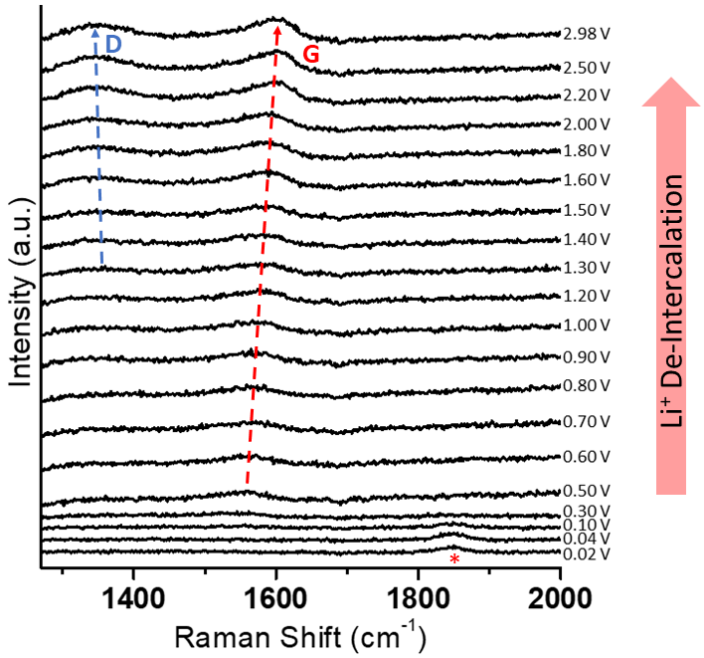

Fig. S5 *In situ* EC Raman spectra of Li-ion de-intercalation for N-rGO electrode (* new Raman peak)

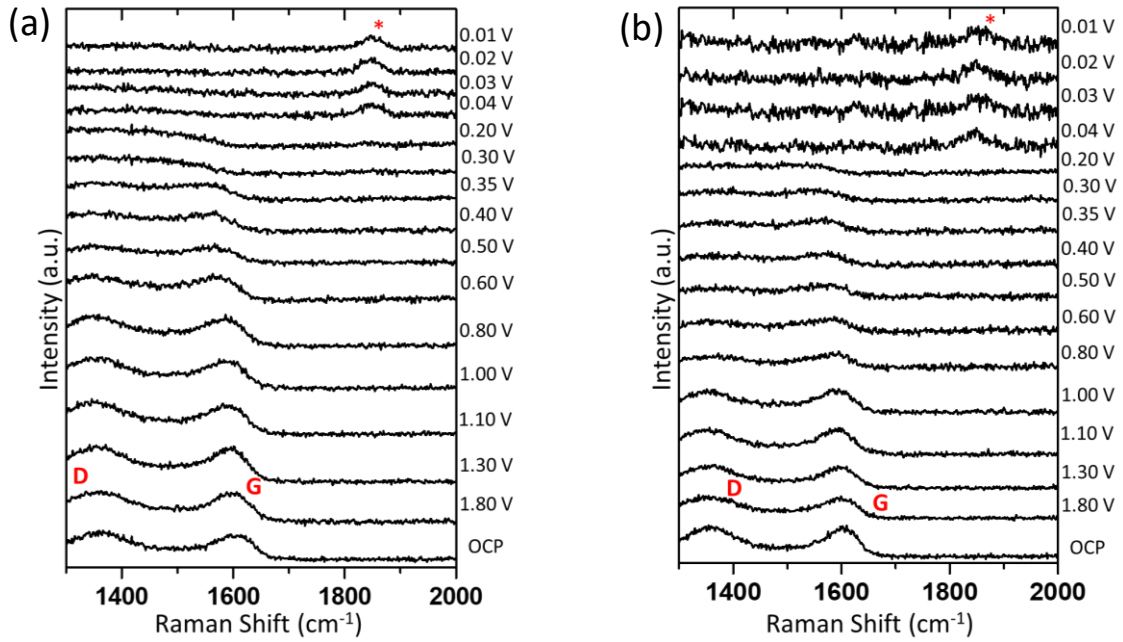

Fig. S6 *In situ* EC Raman spectra of Li^+ intercalation into (a) N-rGO (700) and (b) N-rGO (900) electrode (* new Raman peak observed at 1850 cm^{-1})

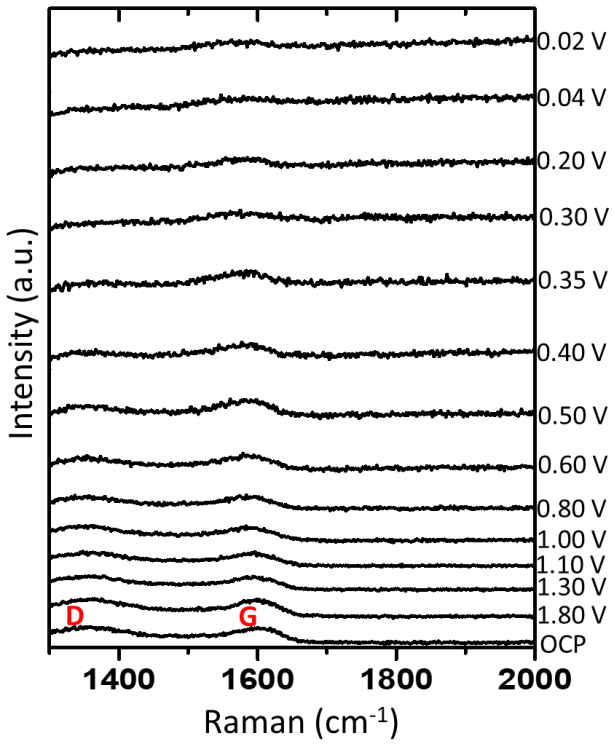

Fig. S7 *In situ* EC Raman spectra of Li^+ intercalation into N-rGO (600)

We believe that the formation of Li_xN species can affect the cyclic stability of the N-rGO electrode, thus 100 cycles of charge-discharge were carried out for rGO and N-rGO anode at C/2 rate in the similar coin cell setup except for the modification of coin cell. It is unrealistic to use the modified coin cell setup for cyclic stability since the epoxy sealing can be weakened with the cycling, which could result in electrolyte evaporation or the air leaking in the cell eventually leading to the degradation of the cell setup.

The cyclic stability of rGO decreased in the initial 50 cycles and later, saturated for the next 50 cycles (Fig. S8 a). This is attributed to the formation of SEI and degradation of rGO anode. In the case of N-rGO, the capacity decreased only during the first 10 cycles and later, increased and stabilized till 100 cycles (Fig. S8 b). The increase in the capacity could be due to the fact that the reversible Li_xN species transforms to an irreversible compound after 10 cycles and participate in the improvement of the cyclability of N-rGO anode. Ma *et al.*[5] and Li *et al.*[6] have reported that the formation of Li_3N suppresses the formation of dendrite on the anode and improves its cyclability. There may be additional underlying factors for the improved cyclability of N-rGO which are yet to be explored. Customized experiments such as cycle-dependent *in situ* EC Raman is required to prove the relation between improved cyclability of N-rGO and Li_xN formation with advanced long-lasting cell setups in which electrolyte leakage during an extensive/sluggish experiment can be avoided.

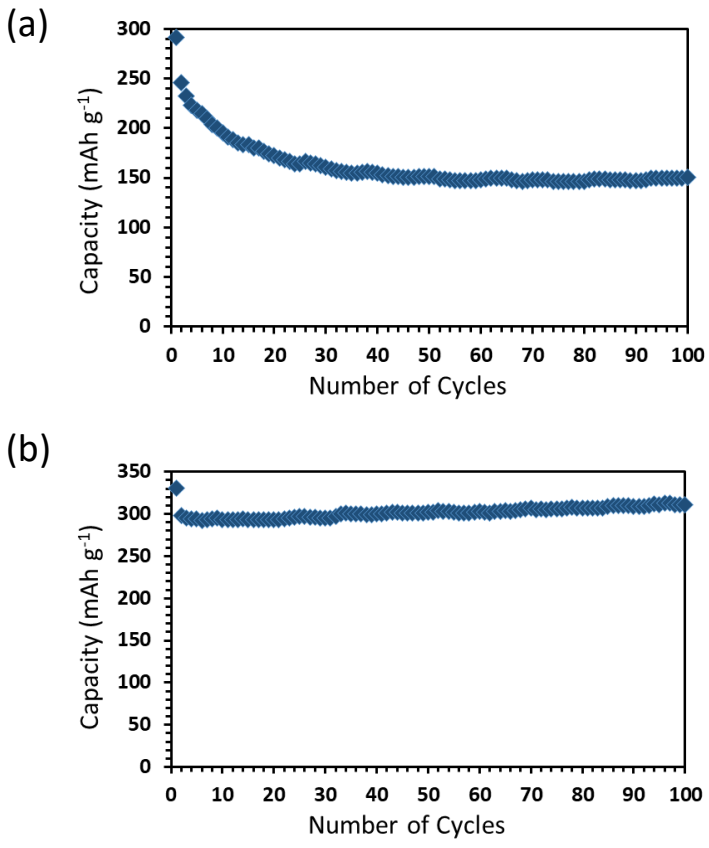

Fig. S8 Cyclic stability of (a) rGO and (b) N-rGO at C/2 rate

To perform XPS of charged N-rGO, the coin cell was charged from OCP to 5 mV, after that the coin cell was transferred and disassembled inside the Ar filled glove box. The charge anode was carefully transferred into the XPS chamber while trying to minimize air exposure.

Fig. S9 (a) shows the N 1s spectrum of charged N-rGO, the spectrum is different from the N 1s spectrum before coin cell assembly in fig. S2. The change in the spectrum shows the formation of different intermediate species on the anode surface. The N 1s spectrum can be fitted with 3 different peaks, a peak at lower binding energy (394.7 eV) could be due to Li_xN, as also reported by Wood *et al.*[7], while the contribution of the other 2 peaks could be from the different functionalities of N and their oxide formation. The Li 1s spectrum was also investigated (fig. S9(b)) to further confirm the formation of Li_xN. The Li 1s spectrum can be fitted with 2 peaks contributing Li metal (Li^0) or lithium oxides and another contribution from Li_xN.[5,7] Fig. S9(c) shows the Li 1s spectrum of charge rGO, the absence of shoulder peak in the lower binding energy, shows the absence of Li_xN formation in the case of charge rGO. Thus the formation of lithium nitride specie (Li_xN) is unlikely in the case of rGO.

The exact interpretation of oxide species from *ex situ* XPS is difficult due to air exposure/contamination during sample transferring from glove box to the XPS chamber, although the points with the lowest oxygen content were selected for the individual scan. Another source of misinterpretation could arise from the fact that the coin cell could self-discharge in the time interval between charged state and XPS investigation.

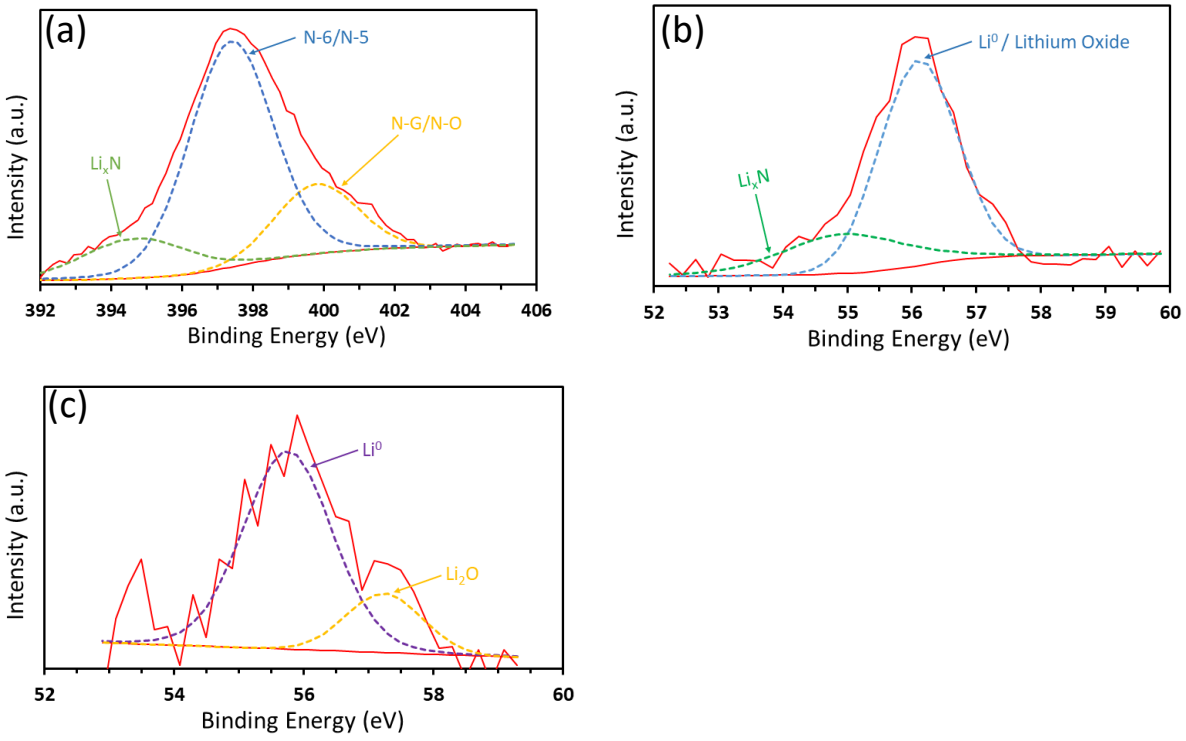

Fig. S9 XPS (a) N 1s, (b) Li 1s scan of N-rGO (800) and (c) Li 1s scan of rGO after charging

Table S1 Positions of Raman peaks for synthetic graphite, rGO, and N-rGO 800 ^{o}C at charging potentials

Potential	Synthetic Graphite		rGO		N-rGO	
	2D (cm^{-1})	G (cm^{-1})	D (cm^{-1})	G (cm^{-1})	D (cm^{-1})	G (cm^{-1})
OCP	2724	1582	1342	1591	1351	1593
1.80	2722	1581	1342	1591	1350	1588
1.60	2723	1581	1341	1591	1356	1587
1.50	2722	1580	1341	1590	1355	1592
1.40	2722	1581	1342	1590	1357	1593
1.30	2724	1581	1339	1588	1353	1594
1.20	2724	1581	1339	1588	1358	1592
1.10	2722	1582	1338	1585	1352	1589
1.00	2724	1581	1339	1584	1353	1587
0.90	2726	1583	1340	1583	1361	1584
0.80	2722	1581	1341	1581	1360	1591
0.70	2722	1580	1339	1580	1364	1591
0.60	2722	1582	1340	1575	1358	1578
0.50	2724	1580	1341	1564	1358	1565
0.40	2719	1585	-	1560	-	1554
0.30	2719	1587	-	1555	-	1538
0.20	2693	1591	-	-	-	-
0.18	2668	-	-	-	-	-
0.16	2668	-	-	-	-	-
0.15	2652	-	-	-	-	-
0.14	2652	-	-	-	-	-
0.12	2652	-	-	-	-	-

Table S2 I_D/I_G ratio for rGO and N-rGO 800 °C with charging potentials

Potential	rGO	N-rGO
	I_D/I_G	I_D/I_G
OCP	1.07	1.04
1.80	1.02	1.05
1.60	1.03	1.06
1.50	1.02	1.01
1.40	1.04	1.04
1.30	1.02	1.06
1.20	1.02	1.03
1.10	1.00	1.02
1.00	0.99	1.04
0.90	0.98	1.01
0.80	1.00	1.03
0.70	0.99	0.97
0.60	1.00	0.95
0.50	1.00	0.92
0.40	0.99	0.92
0.30	-	-
0.20	-	-
0.18	-	-
0.16	-	-
0.15	-	-
0.14	-	-
0.12	-	-

I_D/I_G ratio is used to study the disorder and degradation of electrode material during device operation. The I_D/I_G ratio in the case of rGO and N-rGO remains fairly constant, although a decrease in the ratio from 1.07 to 0.99 and 1.04 to 0.92 is observed for rGO and N-rGO, respectively. This decrease should not be misunderstood as the repairing of defects during Li^+ intercalation because of three main reasons, (1) the decrease in the ratio is very small so there is a possibility of error, (2) the I_D/I_G ratio of rGO is larger than N-rGO after coin cell assembly, which is in contradiction with the ratio calculated before coin cell assembly and (3) the D-peak intensity diminishes earlier than G peak intensity at the extreme potentials (as shown in Table R1). Nakagawa *et al.*[8] and Hardwick *et al.*[9,10] also tried to interpret disorderness on graphite and activated carbon anodes, respectively during device operation by *in-situ* electrochemical Raman spectroscopy. Similar to our investigations, the reports also observed a decrease in the I_D/I_G during intercalation[9,10], however, the decrease was insignificant to make an interpretation and the reason for the decrease was unclear. It was also observed that the ratio can be affected by the type and amount of electrolyte, and the size of cell setup used.[8] Thus, consideration of I_D/I_G ratio after coin cell assembly, in this case, can lead to the

data misinterpretation. Though the decrease in I_D/I_G ratio could be due to the solid electrolyte interface (SEI) formation,[10] the exact explanation is yet to be explored.

References:

1 Z. Q. Li, C. J. Lu, Z. P. Xia, Y. Zhou and Z. Luo, *Carbon N. Y.*, 2007, **45**, 1686.

2 G. Lemes, D. Sebastián, E. Pastor and M. J. Lázaro, *J. Power Sources*, 2019, **438**, 227036.

3 H. Badenhorst, *Carbon N. Y.*, 2014, **66**, 674.

4 A. N. Popova, *Coke Chem.*, 2017, **60**, 361.

5 Y. Ma, L. Li, L. Wang, J. Qian, X. Hu, W. Qu, Z. Wang, R. Luo, S. Fu, F. Wu and R. Chen, *ACS Appl. Mater. Interfaces*, 2020, **12**, 31411.

6 Q. Li, H. Pan, W. Li, Y. Wang, J. Wang, J. Zheng, X. Yu, H. Li and L. Chen, *ACS Energy Lett.*, 2018, **3**, 2259.

7 K. N. Wood and G. Teeter, *ACS Appl. Energy Mater.*, 2018, **1**, 4493.

8 H. Nakagawa, Y. Domi, T. Doi, M. Ochida, S. Tsubouchi, T. Yamanaka, T. Abe and Z. Ogumi, *J. Power Sources*, 2013, **236**, 138.

9 L. J. Hardwick, P. W. Ruch, M. Hahn, W. Scheifele, R. Kötz and P. Novák, *J. Phys. Chem. Solids*, 2008, **69**, 1232.

10 L. J. Hardwick, H. Buqa and P. Novák, *Solid State Ionics*, 2006, **177**, 2801.